SUPPORTING INFORMATION FOR:

Fluorenyl-substituted silole molecules: geometric, electronic, optical, and device properties

Xiaowei Zhan,*[ab] Andreas Haldi,[c] Chad Risko,[a] Calvin K. Chan,[d] Wei Zhao,[d] Tatiana V. Timofeeva,[e] Aleksander Korlyukov,[e] Mikhail Yu. Antipin,[e] Sarah Montgomery,[c] Evans Thompson,[c] Zesheng An,[a] Benoit Domercq,[c] Stephen Barlow,[a] Antoine Kahn,[d] Bernard Kippelen,[c] Jean-Luc Brédas[a] and Seth R. Marder*[a]

[a] *School of Chemistry and Biochemistry and Center for Organic Photonics and Electronics, Georgia Institute of Technology, Atlanta, Georgia 30332, USA. E-mail: seth.marder@chemistry.gatech.edu*

[b] *Beijing National Laboratory for Molecular Sciences and Key Laboratory of Organic Solids, Institute of Chemistry, Chinese Academy of Sciences, Beijing 100080, China. E-mail: xwzhan@iccas.ac.cn*

[c] *School of Electrical and Computer Engineering and Center for Organic Photonics and Electronics, Georgia Institute of Technology, Atlanta, Georgia 30332, USA.*

[d] *Department of Electrical Engineering, Princeton University, Princeton, New Jersey 08544, USA.*

[e] *Department of Natural Sciences, New Mexico Highlands University, Las Vegas, New Mexico 87701, USA.*

CONTENTS

1. Synthesis and characterization

Unless stated otherwise, starting materials were obtained from Aldrich and were used without further purification. 2-Bromo-9,9-dimethylfluorene (**2**),[1] bis(phenylethynyl)diphenylsilane (**3**),[2] 1,1,2,3,4,5-hexaphenylsilole (**0**)[3] and 1,1-bis(9,9-dimethylfluoren-2-yl)-2,3,4,5-tetraphenylsilole (**III**)[1] were prepared according to published procedures.

1-Chloro-1,2,3,4,5-pentaphenylsilole (1). This intermediate was prepared according to a procedure reported by Chen et al.[4] Diphenylacetylene (16.8 mmol, 3.0 g) and clean lithium shavings (14 mmol, 98 mg) were deoxygenated with nitrogen in a 100 mL three-necked round-bottomed flask for 30 min. 15 mL of dry THF was then added. The reaction mixture was stirred at room temperature for 14 h under nitrogen atmosphere. The resultant deep green mixture was diluted with 50 mL of dry THF, and added dropwise to a solution of $PhSiCl_3$ (6.3 mmol, 1.33 g) in 20 mL of dry THF over a period of 0.5 h at room temperature. The brown mixture was stirred at the same temperature for 2 h, and then refluxed for 5 h to give a dark yellow solution. The THF solution of the resultant reactive intermediate **1** was used in situ for the synthesis of siloles without isolation.

1-(9,9-Dimethylfluoren-2-yl)-1,2,3,4,5-pentaphenylsilole (I). To a 250 mL three-necked round-bottomed flask were added **2** (6.3 mmol, 1.72 g) and 20 mL of dry diethyl ether; the solution was deoxygenated with nitrogen for 30 min and cooled to –78 °C. ^{n}BuLi (6.4 mmol, 4 mL, 1.6 M) in hexane was dropwise added over a period of 10 min. The mixture was stirred at the same temperature for 1 h to give a white suspension. The THF solution of **1** was cooled to 0 °C and transferred portionwise into the above organolithium suspension over a period of 30 min. The brown mixture was stirred for 1 h at –78 °C and was gradually warmed to room temperature;

the solution was stirred overnight. The resulting yellow-green solution was washed with water; the organic layer was extracted with diethyl ether and the extracts were dried over anhydrous $MgSO_4$. The solvent was removed and the residue was purified by flash column chromatography on silica gel using 2:1 hexanes/dichloromethane as the eluent. Recrystallization from ethanol gave faintly greenish-yellow, highly blue-fluorescent crystals (1.7 g, 41%, based on **2**). Mp (DSC): 249 °C. ^{1}H NMR (300 MHz, $CDCl_3$): δ 7.72 (m, 4H), 7.66 (s, 1H), 7.64 (d, J = 7.8 Hz, 1H), 7.46-7.32 (m, 6H), 7.04-6.97 (m, 12H), 6.92-6.88 (m, 8H), 1.38 (s, 6H). ^{13}C NMR (75 MHz, $CDCl_3$): δ 156.29, 153.68, 152.80, 141.01, 139.72, 139.60, 138.76, 138.58, 135.94, 134.77, 131.95, 130.44, 129.99, 129.90, 129.64, 129.14, 128.17, 127.67, 127.32, 126.88, 126.27, 125.51, 122.57, 120.24, 119.77, 46.81, 26.97. MS (EI), *m/z* 654.2712 (calcd for $C_{49}H_{38}Si$, 654.2743). Anal. Calcd for $C_{49}H_{38}Si$: C, 89.86; H, 5.85. Found: C, 89.52; H, 5.73%. UV ($CHCl_3$), λ_{max} (ε_{max}) 272 (3.75×10^4), 310 (3.02×10^4), 366 (0.83×10^4) nm (mol^{-1} L cm^{-1}).

1-Fluoren-9-yl-1,2,3,4,5-pentaphenylsilole (II). To a 250 mL three-necked round-bottomed flask were added fluorene (6.0 mmol, 1.0 g) and 20 mL of dry diethyl ether; the solution was deoxygenated with nitrogen for 30 min and cooled to –78 °C. ^{n}BuLi (6.0 mmol, 3.8 mL, 1.6 M) in hexane was dropwise added over a period of 10 min. The mixture was stirred at the same temperature for 1 h to give a golden yellow suspension. The THF solution of **1** was cooled to 0 °C and transferred portionwise into the above organolithium suspension over a period of 30 min. The brown mixture was stirred for 1 h at –78 °C and was gradually warmed to room temperature; the solution was stirred overnight. The resulting yellow-green solution was washed with water; the organic layer was extracted with diethyl ether and the extracts dried over anhydrous $MgSO_4$. The solvent was removed and the residue was purified by flash column chromatography on silica gel using 2:1 hexanes/dichloromethane as eluent. Recrystallization

from ethanol gave faintly greenish-yellow, highly blue-fluorescent crystals (2.3 g, 61%, based on fluorene). Mp (DSC): 218 °C. ^{1}H NMR (300 MHz, $CDCl_3$): δ 7.91 (m, 2H), 7.47 (m, 7H), 7.17 (m, 4H), 6.95 (m, 12H), 6.62 (m, 8H), 4.86 (s, 1H). ^{13}C NMR (75 MHz, $CDCl_3$): δ 156.73, 142.48, 140.77, 138.63, 138.43, 137.17, 135.57, 131.29, 130.20, 129.63, 129.17, 128.17, 127.26, 126.47, 126.10, 125.77, 125.66, 125.24, 124.28, 119.79, 37.72. MS (EI), *m/z* 626.2393 (calcd for $C_{47}H_{34}Si$, 626.2430). Anal. Calcd for $C_{47}H_{34}Si$: C, 90.05; H, 5.47. Found: C, 89.93; H, 5.51%. UV ($CHCl_3$), λ_{max} (ε_{max}) 257 (3.46×10^4), 373 (0.85×10^4) nm (mol^{-1} L cm^{-1}).

1,1,3,4-Tetraphenyl-2,5-bis(9,9-dimethylfluoren-2-yl)-silole (IV). A mixture of lithium shavings (8 mmol, 56 mg) and naphthalene (8.2 mmol, 1.06 g) in dry THF (10 mL) was stirred under nitrogen at room temperature for 5 h to form a deep green suspension of lithium naphthalenide, which was then added dropwise to a solution of **3** (2.0 mmol, 768 mg) in dry THF (5 mL) at room temperature. After stirring for 10 min, the mixture was cooled to 0 °C, and dichloro(*N*,*N*,*N*',*N*'-tetramethylethylenediamine)zinc (8 mmol, 2.0 g) was added as a solid under nitrogen, followed by the dilution with THF (10 mL), to give a black suspension. After stirring for 1 h at room temperature, **2** (4.2 mmol, 1.15 g) and $Pd(PPh_3)_2Cl_2$ (0.2 mmol, 140 mg) were added under nitrogen. The mixture was refluxed and stirred overnight. The resulting yellow-green solution was filtered, and the filtrate was washed with water; the organic layer was extracted with diethyl ether and the extracts were dried over anhydrous magnesium sulfate. Purification by column chromatography on silica gel using 8:1 hexanes/dichloromethane as eluent and recrystallization from methanol afforded a yellow and strong yellow fluorescent solid (0.7 g, 45.4%, based on **3**). Mp (DSC): 218 °C. ^{1}H NMR (300 MHz, $CDCl_3$): δ 7.78 (dd, J = 7.8, 1.5 Hz, 4H), 7.56 (dd, J = 6.6, 1.5 Hz, 2H), 7.45-7.35 (m, 8H), 7.30 (m, 2H), 7.24-7.20 (m, 4H), 7.05 (m, 6H), 6.99 (m, 6H), 6.87 (d, J = 1.2 Hz, 2H), 1.13 (s, 12H). ^{13}C NMR (75 MHz, $CDCl_3$):

δ 156.43, 153.62, 152.79, 139.25, 139.02, 138.37, 136.62, 136.09, 132.10, 130.03, 129.90, 128.30, 128.12, 127.55, 126.70, 126.33, 123.80, 122.35, 119.61, 119.24, 46.31, 26.86. HRMS (EI), *m/z* 770.3308 (calcd for $C_{58}H_{46}Si$, 770.3369). Anal. Calcd for $C_{58}H_{46}Si$: C, 90.34; H, 6.01. Found: C, 90.07; H, 6.09%. UV ($CHCl_3$), λ_{max} (ε_{max}) 285 (3.59×10^4), 402 (2.21×10^4) nm (mol^{-1} L cm^{-1}).

1-(9,9-Dimethylfluorene-2-yl)-2-(trimethylsilyl)acetylene (4). To a 500 mL three-necked round-bottomed flask, **2** (80 mmol, 21.8 g) and Et_3N (300 mL) were added; the mixture was deoxygenated with nitrogen for 30 min. $Pd(PPh_3)_2Cl_2$ (1.6 mmol, 1.12 g) and CuI (4.0 mmol, 760 mg) were added under nitrogen. Then trimethylsilylacetylene (120 mmol, 11.8 g) was added under nitrogen. The black suspension was stirred at 60 °C for 2 days. The mixture was cooled to room temperature, filtered, and insoluble solids were washed with diethyl ether. The solvent was removed and the residue was purified by column chromatography on silica gel using hexanes as eluent to afford pale yellow oil (21.3 g, 92%). ^{1}H NMR (300 MHz, $CDCl_3$): δ7.72-7.68 (m, 1H), 7.63 (m, 1H), 7.54 (m, 1H), 7.47-7.39 (m, 2H), 7.37-7.30 (m, 2H), 1.47 (s, 6H), 0.27 (s, 9H). ^{13}C NMR (75 MHz, $CDCl_3$): δ 153.79, 153.26, 139.49, 138.35, 130.99, 127.61, 126.98, 126.21, 122.55, 121.32, 120.21, 119.71, 105.87, 93.96, 46.87, 27.06, 0.18. HRMS (EI), *m/z* 290.1497 (calcd for $C_{20}H_{22}Si$, 290.1491). Anal. Calcd for $C_{20}H_{22}Si$: C, 82.70; H, 7.63. Found: C, 82.33; H, 7.55%.

(9,9-Dimethylfluorene-2-yl)acetylene (5). 4 (50.0 mmol, 14.5 g) was dissolved in 200 mL methanol. 5 mL aqueous KOH (50 mmol, 2.8 g) was added; the mixture was stirred at room temperature overnight. After the solvent was removed, the residue was dissolved in diethyl ether (200 mL), washed with water, and dried over anhydrous $MgSO_4$. After the solvent was removed, the residue was purified by column chromatography on silica gel using hexanes as eluent to

afford pale yellow oil (9.8 g, 90%). ^{1}H NMR (300 MHz, $CDCl_3$): δ 7.72-7.69 (m, 1H), 7.64 (m, 1H), 7.56 (m, 1H), 7.49-7.39 (m, 2H), 7.36-7.29 (m, 2H), 3.12 (s, 1H), 1.47 (s, 6H). ^{13}C NMR (75 MHz, $CDCl_3$): δ 153.73, 153.33, 139.80, 138.20, 131.10, 127.70, 127.00, 126.35, 122.55, 120.31, 120.25, 119.77, 84.41, 46.86, 27.03. HRMS (EI), *m/z* 218.1095 (calcd for $C_{17}H_{14}$, 218.1096). Anal. Calcd for $C_{17}H_{14}$: C, 93.54; H, 6.46. Found: C, 93.16; H, 6.44%.

1,2-Bis(9,9-dimethylfluorene-2-yl)acetylene (6). To a 500 mL three-necked round-bottomed flask **5** (40 mmol, 8.72 g), **2** (40 mmol, 10.92 g), and Et_3N (250 mL) were added; the mixture was deoxygenated with nitrogen for 30 min. $Pd(PPh_3)_2Cl_2$ (0.8 mmol, 560 mg) and CuI (2.0 mmol, 380 mg) were added under nitrogen. The yellow suspension was stirred at reflux overnight. The black mixture was cooled to room temperature and filtered; insoluble solids were washed with diethyl ether. After the solvent was removed, the residue was purified by column chromatography on silica gel using 8:1 hexanes/dichloromethane as eluent, followed by recrystallization from hexanes to afford white crystals (11.4 g, 70%). ^{1}H NMR (300 MHz, $CDCl_3$): δ 7.72-7.68 (m, 4H), 7.64 (m, 2H), 7.56 (m, 2H), 7.42 (m, 2H), 7.36-7.30 (m, 4H), 1.50 (s, 12H). ^{13}C NMR (75 MHz, $CDCl_3$): δ 153.73, 153.44, 139.22, 138.41, 130.57, 127.55, 127.00, 125.80, 122.55, 121.72, 120.18, 119.88, 90.33, 46.89, 27.12. HRMS (EI), *m/z* 410.2031 (calcd for $C_{32}H_{26}$, 410.2034). Anal. Calcd for $C_{32}H_{26}$: C, 93.62; H, 6.38. Found: C, 93.67; H, 6.42%.

1,1-Diphenyl-2,3,4,5-tetrakis(9,9-dimethylfluoren-2-yl)silole (V). **6** (4 mmol, 1.64 g) and clean lithium shavings (20 mmol, 140 mg) were deoxygenated with nitrogen in a 100 mL three-necked round-bottomed flask for 30 min. 7 mL of dry THF was then added. The reaction mixture was stirred at room temperature for 2 h under nitrogen. The deep green mixture was diluted with 20 mL of dry THF and added dropwise to a solution of Ph_2SiCl_2 (2.0 mmol, 506 mg) in 10 mL of dry THF over a period of 10 min at room temperature. The deep green mixture

was stirred at reflux overnight to give dark yellow solution. The reaction mixture was cooled to room temperature and washed with water; the organic layer was extracted with diethyl ether and dried over anhydrous $MgSO_4$. After the solvent was removed, the residue was purified by flash column chromatography on silica gel using 4:1 hexanes/dichloromethane as eluent, followed by recrystallization from methanol, to afford yellow, strongly yellow-fluorescent solid (1.1 g, 55%). No melting was observed below 350 ºC (DSC). ^{1}H NMR (300 MHz, $CDCl_3$): δ 7.81 (dd, J = 7.8, 1.5 Hz, 4H), 7.54 (dd, J = 6.6, 1.5 Hz, 4H), 7.47-7.35 (m, 10H), 7.26-7.15 (m, 12H), 7.03-6.95 (m, 8H), 1.09 (s, 24H). ^{13}C NMR (75 MHz, $CDCl_3$): δ 157.15, 153.66, 153.03, 139.15, 139.05, 139.00, 138.76, 138.48, 137.26, 136.68, 136.34, 132.33, 130.13, 128.88, 128.37, 128.19, 127.64, 126.77, 126.71, 124.69, 124.05, 122.40, 119.74, 119.65, 119.37, 119.15, 46.39, 46.28, 26.82. HRMS (EI), *m/z* 1002.4608 (calcd for $C_{76}H_{62}Si$, 1002.4621). Anal. Calcd for $C_{76}H_{62}Si$: C, 90.97; H, 6.23. Found: C, 90.57; H, 6.23%. UV ($CHCl_3$), λ_{max} (ε_{max}) 269 (5.43×10^4), 317 (5.91×10^4), 401 (1.39×10^4) nm (mol^{-1} L cm^{-1}).

^{1}H and ^{13}C NMR spectra were measured on a Varian Mercury 300 spectrometer using tetramethylsilane (TMS; δ = 0 ppm) as an internal standard. Mass spectra were measured on a VG Instruments 70-SE using the electron impact (EI) mode. Elemental analyses were carried out by Atlantic Microlabs using a LECO 932 CHNS elemental analyzer. Solution (chloroform) and thin-film (on quartz substrate) UV-vis absorption spectra were recorded with a Varian Cary 5E UV-vis-NIR spectrophotometer, while solution (chloroform) and thin-film PL spectra were recorded with a Shimadzu FP-5301PC spectrofluorometer. Electrochemical measurements were carried out under nitrogen on a deoxygenated solution of tetra-*n*-butylammonium hexafluorophosphate (0.1 M) in 1:1 (by volume) acetonitrile / toluene using a computer-

controlled BAS 100B electrochemical analyzer, a glassy-carbon working electrode, a platinum-wire auxiliary electrode, and a Ag wire anodized with AgCl as a pseudo-reference electrode. Potentials were referenced to the ferrocenium / ferrocene ($FeCp_2^{+/0}$) couple by using ferrocene as an internal standard. Thermogravimetric analysis (TGA) measurements were performed with a Shimadzu thermogravimetric analyzer (model TGA-50) under a nitrogen flow at a heating rate of 10 °C/min. Differential scanning calorimetry (DSC) measurements were performed with a Shimadzu differential scanning calorimeter (model DSC-50) under a nitrogen flow at a heating rate of 10 °C/min. XRD data for films of siloles were collected on a Scintag X1 diffractometer with a Cu Kα source (λ = 1.5406 Å) in a continuous scan mode with a step size of 0.02 degree. Polarizing microscopy images were obtained using an Olympus BX51 microscope equipped with an Olympus U-TU1 X digital camera and an Instec STC200 hot stage.

2. Single-crystal growth and X-ray crystallographic analysis

Single crystals of compounds **II** and **IV** were grown from a chloroform-ethanol mixture as yellow prisms and needles, respectively. X-ray diffraction measurements for **II** and **IV** were carried out with a Syntex $P2_1$ diffractometer. Crystallographic data, details of data collection and structure refinement are presented in Table S1. The structures were solved by direct methods and refined by a full-matrix least-squares technique against F^2 in the anisotropic-isotropic approximation. The hydrogen atoms were located from difference electron density syntheses and refined using a rigid body model. All calculations were performed using the SHELXTL PLUS 5.10 program package.[5] In their crystals, molecules **II** and **IV** have symmetry C_1 and C_2, respectively.

Table S1 Crystal data and experimental conditions for compounds **II** and **IV**

	II	**IV**
Molecular formula	$C_{47}H_{34}Si$	$C_{58}H_{46}Si$
Formula weight	626.83	771.04
Dimension/mm	$0.3 \times 0.1 \times 0.1$	$0.4 \times 0.1 \times 0.1$
Crystal system	Monoclinic	Orthorhombic
Space group	$P2_1/c$	Pbcn
a/Å	13.448(4)	17.034(5)
b/Å	10.218(2)	10.422(2)
c/Å	25.111(6)	24.427(8)
β/°	97.34(2)	90.00
Volume/Å^3	3422.2	4336(2)
Z	4	4
ρ_{calc}/g cm^{-3}	1.217	1.181
Temperature/K	120	203
Scan type	Θ/2Θ	Θ/2Θ
2θ max/º	29.07	26.06
Radiation, λ(Mo-Kα)/Å	0.71073	0.71073
Linear absorption (μ)/cm^{-1}	1.02	0.93
Absorption correction	None	None
F(000)	1320	1632
Total refl. (R_{int})	9450 (0.0336)	4482 (0.1165)
Number of independent refl.	9091	4224
Number of independent refl. with I>2(σ)	6672	1562
Parameters	433	267
wR_2 [all reflections]	0.0998	0.1229
R_1 [I>2(σ)]	0.0416	0.0623
Goodness-of-fit	1.038	0.937
ρ_{max}/ρ_{min}/eÅ^{-3}	0.610/-0.331	0.262/-0.322

3. PES and IPES data collection

Materials were loaded into individual pyrolytic boron nitride (PBN) crucibles and placed in a vacuum growth chamber with a base pressure of 10^{-9} Torr. The sources were thoroughly

degassed prior to use. Approximately 2-5 nm thick films of each material were deposited by thermal sublimation onto separate Si(100) substrates that were pre-coated with a 5 nm Ti adhesion layer and 120 nm of Au. The Si/Ti/Au substrates were cleaned with acetone and methanol prior to mounting and loading into vacuum. The 0.1 nm/s rate of deposition and film thicknesses were determined by a quartz crystal microbalance assuming a material density of 1.5 g/cc.

After thin film growth, samples were transferred without breaking vacuum into an analysis chamber with a base pressure of 10^{-10} Torr and analyzed with PES and IPES. PES was performed using a non-monochromatized differentially pumped He discharge lamp (Specs) with primary lines at $h\nu$ = 21.22 eV (He I) and $h\nu$ = 40.8 eV (He II). The photoemitted electrons were analyzed with a cylindrical analyzer with an experimental resolution of 0.15 eV. IPES was conducted using a Kimbal Physics electron gun as the source and an isochromatic photon detector centered at 9.2 eV. The experimental resolution of the IPES was 0.5 eV. In order to limit damage induced by the electron gun, the defocused beam current was limited to 1 $\mu A/cm^2$, and subsequent scans for averaging were taking at various spots within the sample area.

The PES and IPES energy scales were aligned at the Fermi-level (E_F) of the two measurement systems, which were determined by measuring the position of E_F in PES and IPES on a freshly deposited Au reference sample. The position of the vacuum level (E_{vac}) was found by adding the photon energy to the onset of photoemission.[6] The adiabatic ionization energy and electron affinity were then determined by the distance from E_{vac} to the leading edge of the HOMO and LUMO features, respectively.[7]

4. Preparation of electroluminescence devices

For OLEDs with solution-processed organic layers, 35 nm-thick films of the crosslinkable hole-transport material **7**[8] (Fig. S1) were spin-coated from toluene onto air-plasma-treated indium tin oxide (ITO) coated-glass substrates with a sheet resistance of 20 Ω/ (Colorado Concept Coatings, L.L.C.). Films were crosslinked using a standard broad-band UV light with a 0.7 mW/cm^2 power density for 1 min. Subsequently, a 35 nm-thick emissive layer was spin-coated from a toluene solution of the silole derivative blended with polystyrene (PS) in a weight ratio of 4:1.

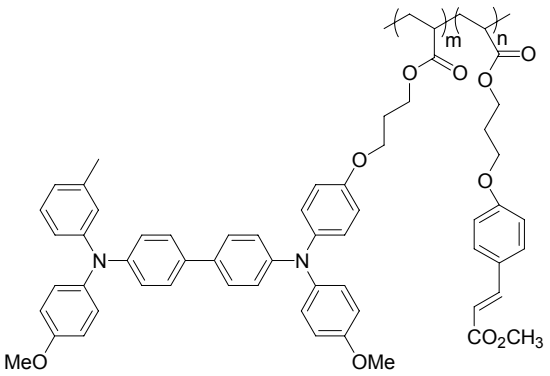

Fig. S1 Chemical structure of **7**.

For thermal evaporation, *N,N'*-bis(*m*-tolyl)-*N,N'*-diphenyl-1,1'-biphenyl-4,4'-diamine (TPD) and tris-(8-hydroxyquinolinato-N,O) aluminum (Alq_3) were first purified using gradient zone sublimation. The silole molecules were purified by column chromatography and recrystallization. Films of 35 to 40 nm were then thermally evaporated at a rate of 1 Å/s and at a pressure below 1×10^{-7} Torr onto air-plasma-treated ITO-coated glass substrates with a sheet resistance of 20 Ω/ (TPD) or on the previously deposited organic layer (silole and Alq_3). 1 nm of lithium fluoride (LiF) and a 200 nm-thick aluminum cathode were vacuum-deposited at a

pressure below 1×10^{-6} Torr and at rates of 0.1 Å/s and 2 Å/s, respectively. A shadow mask was used for the evaporation of the metal to form five devices per substrate with an area of 0.1 cm^2 each. At no point during fabrication were the devices exposed to atmospheric conditions. The testing was done immediately after the deposition of the metal cathode in inert atmosphere without exposing the devices to air.

5. Computational details

Geometry optimizations of the neutral, radical-anion, and radical-cation states were performed at DFT level using the B3LYP functional[9-11] and a 6-31G* split valence plus polarization basis set. Excitation energies for the low-lying excited states were calculated with time-dependent density functional theory (TD-DFT). All DFT calculations were performed with Gaussian98 (revision A.11).[12]

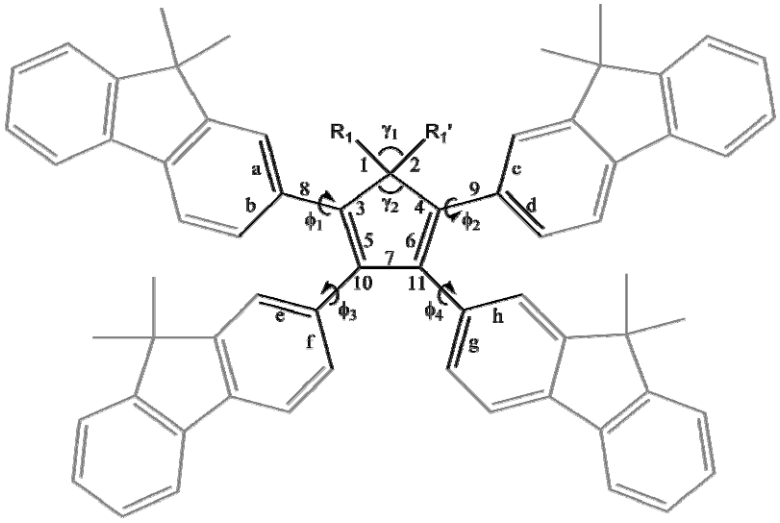

Fig. S2 Bond and angle numbering scheme.

Table S2 Selected B3LYP/6-31G*-calculated geometric parameters for **I**

	Neutral	Anion	Δ(a-n)	Cation	Δ(c-n)
Bond length/Å					
1	1.886	1.914	0.028	1.870	-0.016
2	1.889	1.912	0.023	1.876	-0.013
3	1.889	1.863	-0.026	1.907	0.018
4	1.890	1.864	-0.026	1.907	0.017
5	1.367	1.417	0.050	1.408	0.041
6	1.368	1.418	0.050	1.407	0.039
7	1.513	1.454	-0.059	1.463	-0.050
8	1.479	1.463	-0.016	1.451	-0.028
a	1.409	1.420	0.011	1.421	0.012
b	1.408	1.419	0.011	1.420	0.012
9	1.479	1.462	-0.017	1.451	-0.028
c	1.409	1.420	0.011	1.421	0.012
d	1.408	1.421	0.013	1.420	0.012
10	1.492	1.487	-0.005	1.486	-0.006
e	1.404	1.409	0.005	1.406	0.002
f	1.405	1.409	0.004	1.406	0.001
11	1.492	1.487	-0.005	1.486	-0.006
g	1.404	1.409	0.005	1.406	0.002
h	1.405	1.409	0.004	1.406	0.001
Bond angle/°					
γ_1	111.6	106.6	-5.0	114.5	2.9
γ_2	92.5	93.9	1.4	90.3	-2.2
Dihedral angle/°					
ϕ_1	48.1	39.6	-8.5	33.3	-14.8
ϕ_2	47.3	39.5	-7.8	32.3	-15.0
ϕ_3	57.9	55.4	-2.5	59.3	1.4
ϕ_4	57.8	55.4	-2.4	59.4	1.6

Table S3 Selected X-ray crystallographic and B3LYP/6-31G*-calculated geometric parameters for **II**

	X-ray	Calc.				
	Neutral	Neutral	Anion	Δ(a-n)	Cation	Δ(c-n)
Bond length/Å						
1	1.8973(19)	1.930	1.970	0.040	1.920	-0.010
2	1.8677(14)	1.896	1.923	0.027	1.883	-0.013
3	1.8672(13)	1.892	1.860	-0.032	1.908	0.016
4	1.8750(14)	1.888	1.867	-0.021	1.906	0.018
5	1.3569(18)	1.365	1.420	0.055	1.410	0.045
6	1.3601(18)	1.367	1.417	0.050	1.407	0.040
7	1.5026(18)	1.510	1.447	-0.063	1.457	-0.053
8	1.4805(18)	1.480	1.457	-0.023	1.449	-0.031
a	1.3926(19)	1.409	1.421	0.012	1.421	0.012
b	1.3983(18)	1.409	1.423	0.014	1.423	0.014
9	1.4800(18)	1.480	1.463	-0.017	1.449	-0.031
c	1.394(2)	1.408	1.421	0.013	1.423	0.015
d	1.400(2)	1.408	1.421	0.013	1.424	0.016
10	1.4921(17)	1.497	1.492	-0.005	1.188	-0.009
e	1.395(2)	1.402	1.409	0.007	1.406	0.004
f	1.389(2)	1.403	1.407	0.004	1.408	0.005
11	1.4903(18)	1.497	1.499	0.002	1.495	-0.002
g	1.392(2)	1.402	1.405	0.003	1.401	-0.001
h	1.390(2)	1.403	1.404	0.001	1.404	0.001
Bond angle/°						
γ_1	108.76(6)	110.9	106.5	-4.4	115.1	4.2
γ_2	92.80(6)	93.0	94.5	1.5	90.7	-2.3
Dihedral angle/°						
ϕ_1	32.36(17)	43.9	31.9	-12.0	26.5	-17.4
ϕ_2	56.29(16)	43.9	19.6	-24.3	25.0	-18.9
ϕ_3	59.51(17)	79.1	66.3	-12.8	63.6	-15.5
ϕ_4	54.97(18)	77.9	84.8	6.9	86.9	9.0

Table S4 Selected X-ray crystallographic and B3LYP/6-31G*-calculated geometric parameters for **IV**

	X-ray	calc.				
	Neutral	Neutral	Anion	Δ(a-n)	Cation	Δ(c-n)
Bond length/Å						
1	1.886(4)	1.890	1.912	0.022	1.882	-0.008
2	1.886(4)	1.890	1.912	0.022	1.882	-0.008
3	1.875(4)	1.892	1.874	-0.018	1.907	0.015
4	1.875(4)	1.892	1.874	-0.018	1.907	0.015
5	1.373(5)	1.368	1.413	0.045	1.404	0.036
6	1.373(5)	1.368	1.413	0.045	1.404	0.036
7	1.455(8)	1.510	1.455	-0.055	1.463	-0.047
8	1.476(6)	1.477	1.456	-0.021	1.446	-0.031
a	1.422(5)	1.413	1.426	0.013	1.429	0.016
b	1.405(5)	1.411	1.425	0.014	1.427	0.016
9	1.476(6)	1.477	1.456	-0.021	1.446	-0.031
c	1.422(5)	1.413	1.426	0.013	1.429	0.016
d	1.405(5)	1.411	1.425	0.014	1.427	0.016
10	1.523(5)	1.493	1.489	-0.004	1.491	-0.002
e	1.369(6)	1.404	1.408	0.004	1.405	0.001
f	1.392(5)	1.395	1.408	0.013	1.405	0.010
11	1.523(5)	1.493	1.489	-0.004	1.491	-0.002
g	1.369(6)	1.404	1.408	0.004	1.405	0.001
h	1.392(5)	1.395	1.408	0.013	1.405	0.010
Bond angle/°						
γ_1	109.6(2)	110.4	107.1	-3.3	113.2	2.8
γ_2	91.8(3)	92.3	93.4	1.1	90.9	-1.4
Dihedral angle/°						
ϕ_1	-36.7(5)	45.6	34.9	-10.7	27.4	-18.2
ϕ_2	-36.7(5)	45.6	34.9	-10.7	27.4	-18.2
ϕ_3	-61.2(7)	60.1	58.5	-1.6	63.8	3.7
ϕ_4	-61.2(7)	60.1	58.5	-1.6	63.8	3.7

Table S5 Selected B3LYP/6-31G*-calculated geometric parameters for **V**

	Neutral	Anion	Δ(a-n)	Cation	Δ(c-n)
Bond length/Å					
1	1.890	1.910	0.020	1.886	-0.004
2	1.890	1.910	0.020	1.878	-0.012
3	1.891	1.873	-0.018	1.904	0.013
4	1.891	1.873	-0.018	1.902	0.011
5	1.367	1.410	0.043	1.400	0.033
6	1.367	1.410	0.043	1.405	0.038
7	1.511	1.459	-0.052	1.465	-0.046
8	1.477	1.458	-0.019	1.447	-0.030
a	1.413	1.423	0.010	1.427	0.014
b	1.411	1.425	0.014	1.426	0.015
9	1.477	1.458	-0.019	1.443	-0.034
c	1.413	1.423	0.010	1.427	0.014
d	1.411	1.425	0.014	1.429	0.018
10	1.492	1.486	-0.006	1.495	0.003
e	1.407	1.413	0.006	1.404	-0.003
f	1.408	1.412	0.004	1.409	0.001
11	1.492	1.486	-0.006	1.489	-0.003
g	1.408	1.413	0.005	1.412	0.004
h	1.407	1.412	0.005	1.407	0.000
Bond angle/°					
γ_1	110.1	106.9	-3.2	113.0	2.9
γ_2	92.3	93.1	0.8	91.1	-1.2
Dihedral angle/°					
ϕ_1	47.5	38.0	-9.5	28.2	-19.3
ϕ_2	47.5	38.0	-9.5	23.9	-23.6
ϕ_3	60.5	58.3	-2.2	81.8	21.3
ϕ_4	60.5	58.3	-2.2	67.9	7.4

6. X-ray diffraction pattern for IV

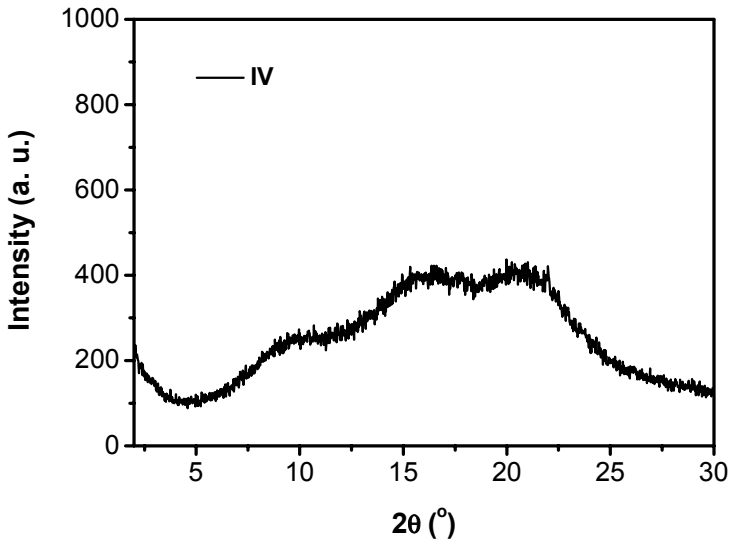

Fig. S3 X-ray diffraction pattern for a thin film of **IV** after heating to 248 °C then cooling down to room temperature.

7. References for supporting information

1 X. Zhan, C. Risko, F. Amy, C. Chan, W. Zhao, S. Barlow, A. Kahn, J. L. Brédas and S. R. Marder, *J. Am. Chem. Soc.*, 2005, **127**, 9021.

2 M. Malenthal, M. Hellmann, C. P. Haber, L. A. Hymo, S. Carpenter and A. J. Carr, *J. Am. Chem. Soc.*, 1954, **76**, 6392.

3 B. Z. Tang, X. W. Zhan, G. Yu, P. P. S. Lee, Y. Q. Liu and D. B. Zhu, *J. Mater. Chem.*, 2001, **11**, 2974.

4 J. Chen, C. C. W. Law, J. W. Y. Lam, Y. Dong, S. M. F. Lo, I. D. Williams, D. Zhu and B. Z. Tang, *Chem. Mater.*, 2003, **15**, 1535.

5 G. M. Sheldrick, SHELXTL-97 V5.10, Bruker AXS, Madison, WI-53719, USA, 1997.

6 D. Cahen and A. Kahn, *Adv. Mater.*, 2003**, 15**, 271.

7 C. Shen, A. Kahn and I. G. Hill, in *Conjugated polymer and molecular interfaces: science and technology for photonic and optoelectronic applications*, ed. W. R.

Salaneck, K. Seki, A. Kahn and J. J. Pireaux, Marcel Dekker, Incorporated, New York, 2002, pp. 351-400.

8 B. Domercq, R. D. Hreha, Y. D. Zhang, N. Larribeau, J. N. Haddock, C. Schultz, S. R. Marder and B. Kippelen, *Chem. Mater.*, 2003, **15**, 1491.

9 A. D. Becke, *Phys. Re*v. *A*, 1988, **38**, 3098.

10 A. D. Becke, *J. Chem. Phys.*, 1993, **98**, 5648.

11 C. Lee, W. Yang and R. G. Parr, *Phys. Re*v. *B*, 1988, **37**, 785.

12 M. J. Frisch, G. W. Trucks, H. B. Schlegel, G. E. Scuseria, M. A. Robb, J. R. Cheeseman, V. G. Zakrzewski, J. A. Montgomery, R. E. Stratmann, J. C. Burant, S. Dapprich, J. M. Millam, A. D. Daniels, K. N. Kudin, M. C. Strain, O. Farkas, J. Tomasi, V. Barone, M. Cossi, R. Cammi, B. Mennucci, C. Pomelli, C. Adamo, S. Clifford, J. Ochterski, G. A. Petersson, P. Y. Ayala, Q. Cui, K. Morokuma, P. Salvador, J. J. Dannenberg, D. K. Malick, A. D. Rabuck, K. Raghavachari, J. B. Foresman, J. Cioslowski, J. V. Ortiz, A. G. Baboul, B. B. Stefanov, G. Liu, A. Liashenko, P. Piskorz, I. Komaromi, R. Gomperts, R. L. Martin, D. J. Fox, T. Keith, M. A. Al-Laham, C. Y. Peng, A. Nanayakkara, M. Challacombe, P. M. W. Gill, B. Johnson, W. Chen, M. W. Wong, J. L. Andres, C. Gonzalez, M. Head-Gordon, E. S. Replogle and J. A. Pople, *Gaussian98, Rev. A.11*, 1998.